6450 *Macromolecules* **2010**, *43*, 6450–6462
DOI: 10.1021/ma100626d

Macromolecules
ARTICLE

Effect of Dilution on Structure and Properties of Polyurethane Networks. Pregel and Postgel Cyclization and Phase Separation

Miroslava Dušková-Smrčková,*,† Helena Valentová,‡ Andrea Ďuračková,† and Karel Dušek†

†*Institute of Macromolecular Chemistry, Academy of Sciences of the Czech Republic Prague, Czech Republic, and* ‡*Department of Macromolecular Physics, Faculty of Mathematics and Physics, Charles University, Prague, Czech Republic*

Received March 23, 2010; Revised Manuscript Received June 1, 2010

ABSTRACT: Bi-, tri-, and tetrafunctional star-shaped polyol precursors were cross-linked with a star-shaped triisocyanate and the effect of the presence of diluent during network formation on the gel-point conversion, α_{crit}, and on the equilibrium elastic modulus was studied. The dependence of α_{crit} on reciprocal concentration of functional groups, $1/c_0$, was fairly linear and extrapolated for $1/c_0 \rightarrow 0$ well to the value calculated for the ring-free system using the branching theory. The decrease of the equilibrium modulus and of the associated concentration of elastically active network chains (EANC) in dependence on the volume fraction of polymerizable compounds (solids), memory factor ϕ_2^0, was curved downward and extrapolated to the limiting dilution of the system at which no gel was formed at full conversion of functional groups. Some highly diluted samples exhibited phase separation in the form of macrosyneresis (expulsion of excess solvent as bulk phase) which affected the memory factor ϕ_2^0. The situation was analyzed from the point of view of changes of thermodynamic stability of the system during cross-linking and a procedure was developed to find a correct value of ϕ_2^0 in such cases. A linear correlation was found between the shift of the gel-point conversion and the change of intermolecular conversion corresponding to experimental changes of the concentration of EANCs. The dependence of the concentration of EANCs on intermolecular conversion was obtained by branching theory. It has been shown that it is possible to estimate the decrease of effective cross-link density caused by dilution during network formation from the shift of the gel-point conversion.

Introduction

The cross-linked state of macromolecular matter is a necessary condition for shape memory, good thermomechanical properties and durability of thermosets, and limited swelling and reversible elasticity of elastomers and gels. Often, cross-linking is carried out in the presence of a nonpolymerizable compound which is not chemically bound to the forming network—a diluent. The presence of diluent plays an important role. For instance, in high-solids coatings it makes the formation of a coating film possible by adjusting the viscosity of the binder and enabling the functional groups to react; in hydrogels, water as diluent is the natural environment in which chemical and physical gels function and operate. Also, diluents are used to produce porous polymeric materials.

The effect of presence of a diluent is manifold:[1−7] increasing amount of diluent (1) enhances the intramolecular cross-linking at the expense of intermolecular bond formation, (2) weakens interchain interactions, (3) may cause or contribute to formation of static fluctuations in segment densities, and (4) can give rise to one of the forms of phase separation.

Each of these effects of diluent has been a subject of studies since several decades ago. The most important effect of dilution is the increase of cyclization. Ring-closing arises from bond formation between functional groups already connected by a sequence of bonds. Before the gel point, an intramolecular bond is defined unambiguously: by its formation the molecular weight does not increase (cf., Figure 1). The extent of cyclization depends on many factors, but primarily on the number of functional groups and topological distances between them, flexibility of connecting paths, volume concentration of functional groups, cross-link functionality, and mechanism of the cross-linking reaction. The fraction of bonds "wasted" in closing cycles ranges from a few percent[3,8] (or even less) to moderate extents (several tens of percent),[9,10] and to predominating cyclization like in the early stages of chain cross-linking copolymerization.[3,11−15]

The gel existing beyond the gel point contains many cycles—closed circuits that are composed of elastically active network chains (EANCs) contributing to equilibrium elasticity. Yet, there are some cycles (loops) that are elastically inactive and do not contribute to equilibrium elasticity. Some of the cyclic structures contribute only partially. As the cross-linking reaction proceeds, some of the elastically inactive loops are transferred into states in which the chains acquire elastic activity (Figure 2).

Experimentally, cyclization is manifested by shift of the gel-point conversion to higher values and beyond the gel point by lowering of the equilibrium modulus. One of the consequences of weakening of interchain interactions by dilution is the decrease of the number of possibly existing trapped entanglements. Also, it makes the fluctuations of junctions more free (cf., e.g., the Flory−Erman junction-fluctuation model[4]), and diminishes the interchain excluded volume[4] (cf., e.g., tube models). Experimentally, weakening of interchain interactions assists the system to approach simple stress−strain behavior (e.g., decrease and possible disappearance of the C_2 constant in the Mooney−Rivlin equation). Weakening of interchain interactions is caused also by swelling of the network after it has been formed.

Static inhomogeneities have been recorded by scattering techniques in a number of (highly) swollen gels, especially hydrogels.[6,16] They arise from associating sites of network chains fixed

*Corresponding author.

 Published on Web 07/12/2010

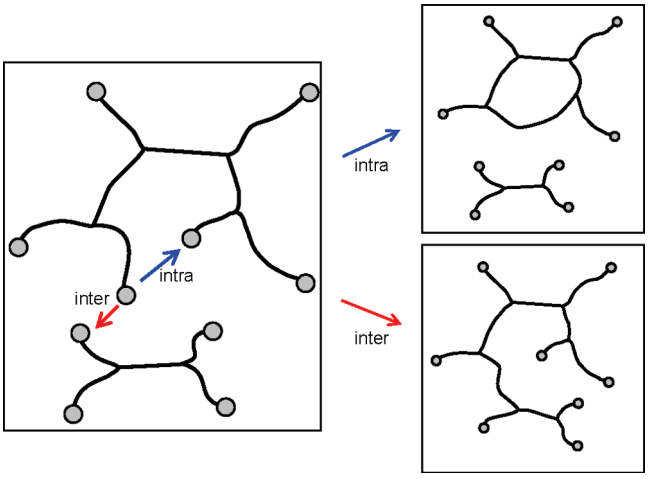

Figure 1. Inter- and intramolecular reaction during cross-linking. The circles represent unreacted functional groups.

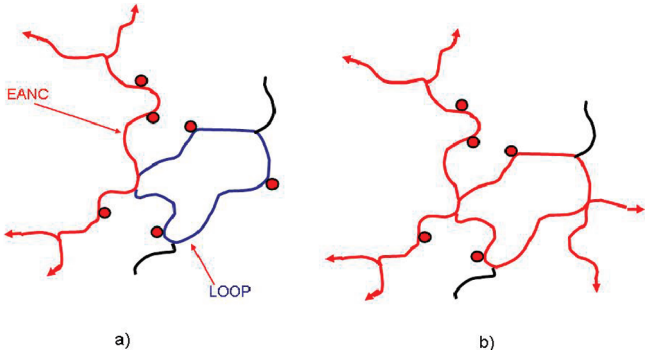

Figure 2. Elastically inactive cycle (a) and transformed cyclic structure taking part in elastic response (b). The circles represent unreacted functional groups, red line the elastically active chain, blue line the elastically inactive chain, and black line the pending chain. Arrows mean continuation to infinite network structure.

by cross-linking or from inhomogeneous cross-linking. However, inhomogeneities are not inherent attributes of gels. Recently, it was found[17−20] that hydrogels prepared from star-shaped precursors did not show any inhomogeneities. Fixed fluctuation in segment and cross-link densities are frequently absent or weak in step-growth networks compared to chain-growth systems with fast propagation.

Under certain conditions, the cross-linking system looses its thermodynamic stability and phase separates. In the region well beyond the gel point, where the sol fraction is negligible, the coexisting phases are composed of swollen gel and diluent, respectively, closer to the gel point the sol is redistributed between the gel and liquid phases. Whether the phase separation occurs in the form of microsyneresis (dispersion of one phase in the other one, or co-continuous interdispersion of both phases on nano- to microscale) or macrosyneresis (bulk gel and liquid phases) depends on the gel strength.[1,2,21] Microsyneresis is characteristic of the region near the gel point whereas macrosyneresis occurs at higher conversion well beyond the gel point.

Evolution of network structure has been modeled using various theoretical approaches of which the statistical method of assemblage of branched and cross-linked structures from smaller fragments can best utilize the information supplied by chemists on kinetics and mechanism of bond formation. This information includes various distributions (of molecular weight, functionality, and group reactivity) that are characteristic of precursors used in practice. The statistical models are well elaborated for ring-free systems. However, in the majority of systems, cyclization is important and perturbation methods to the ring-free system as reference have been utilized (e. g., Rolfes−Ahmad−Stepto rate theory or spanning-tree model) with moderate success in the pregelation region (cf., e.g., refs 3 and 22−27). These methods are based on conformational probability of meeting of two functional groups already connected by a path of bonds relative to the probability of meeting of groups residing on different molecules (the Stockmayer−Jacobson −3/2 law is usually a good approximation). However, for stronger cyclization, the assessment of cyclization probability is difficult. The situation beyond the gel point and formation of elastically inactive cycles (elastically inactive cross-links−IEC) are much more complicated. The modeling efforts concentrated on adaptation of the spanning-tree model considering also an IEC activation process by which an IEC is transformed into elastically active chains.[24,25] Similarly, Stepto et al.[28,29] generated elastically inactive loops by Monte Carlo method and estimated the effect of cyclization on modulus of elasticity. These models give good guidance for existing systems, but none of them in their present state is sufficiently predictive for newly developed systems.

In this contribution, we have determined the effect of diluent on the gel-point conversion and small-strain modulus of elasticity as well as some viscoelastic properties of several polyurethane networks obtained by endlinking of star-shaped precursors. We have focused on interrelations between the lowering of the equilibrium modulus due to dilution and the shift of the critical gel-point conversion caused by dilution. The clue to this interrelation has been supplied by the ring-free branching theory in which transformation of the branching system into gel and formation of elastically active chains are a function of intermolecular conversion of functional groups. The studied systems have provided several instances of cross-linking induced phase separation in the form of macrosyneresis. These phenomena have been discussed in terms of thermodynamics of swollen polymer networks. Phase separation also determines the coiling state of network chains.

Experimental Section

Chemicals. The diluents, solvents, and the other chemicals were of reagent grade or analytical grade supplied by Sigma-Aldrich Co. and used as received. From those used as diluents, if necessary, water was removed by molecular sieves, so that its content did not exceed 0.01 wt %. The diluents were stored over molecular sieves with pore size 4 Å. As isocyanate components, trimers of 1,6-diisocyanatohexane, Desmodur N3300 and Desmodur N3600 kindly provided by Bayer Co. were used. Their characterization is described below.

Hydroxy-Functional Precursors. The tetrafunctional star (4-f STAR, Scheme 1a), was an oligoester with primary OH groups located at the arm ends and was prepared by reaction of a pentaerythritol with (substituted) hexahydrophthalic anhydride and subsequently functionalized with ethylene oxide as described in ref 30. Its number-average molecular weight was 942 g/mol and its number-average functionality determined from mass spectroscopy was $\langle f_{OH}\rangle_1 = 3.96 \approx 4.0$.

Polycaprolactone triols (PCLT 300, PCLT 900) and polycaprolactone diol (PCLD 1250) were purchased from Sigma-Aldrich. Their molecular weights were approximately 300, 900, and 1250 g/mol (supplier information). The structures of PCLTs and PCLD are depicted in the Scheme 1. For designing the model networks, the equivalent weights were calculated from OH number values. The OH number was determined using a standard procedure of quantitative acetylation of OH groups by acetic acid anhydride and potentiometric titration of the excess acetic acid. The functionality of PCL

Scheme 1. Structure of Precursors: (a) 4-f STAR; (b) Polycaprolactone Triols; (c) Polycaprolactone Diol; (d) Trimer of 1,6-Diisocyanatohexane

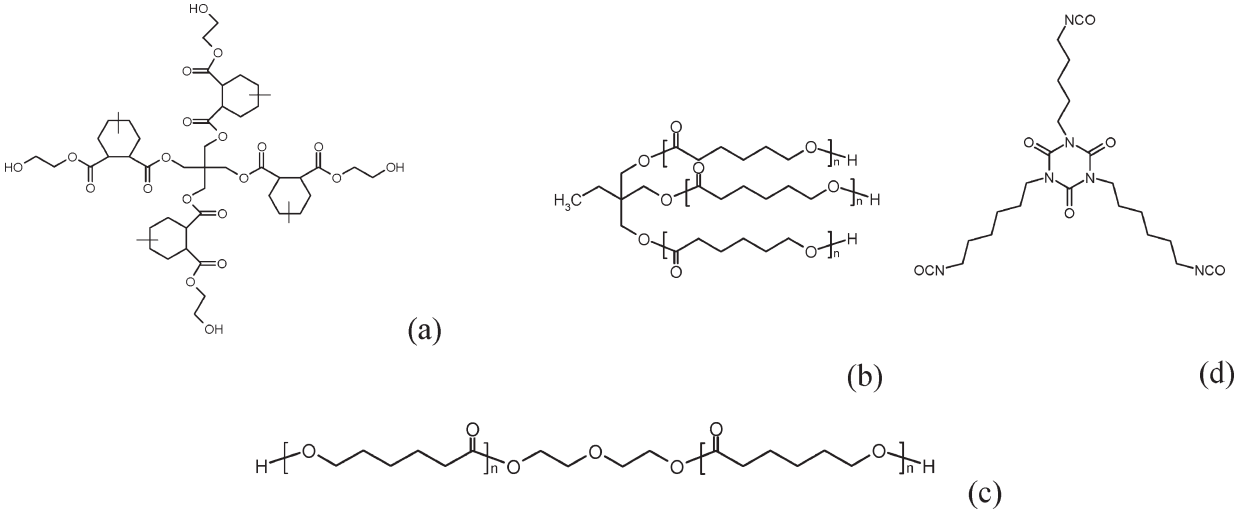

Table 1. Composition of a Sample of Desmodur N3300 Deactivated by Benzyl Alcohol as Determined by MS[a]

m/*z*, Da	composition	relative intensity	assumed structure	functionality
549	$2HDI + 2BzOH + Na^+ - CO_2 + H_2O$	5	I	2
851	$3HDI + 3BzOH + Na^+$	100	II	3
1274	$5HDI + 4BzOH + Na^+ - Na^+$	40	III	4
1296	$5HDI + 4BzOH + Na^+$	22	III	4
1412	$6HDI + 4BzOH + Na^+ - 2CO_2 + 2H_2O$	4	IV	4
1438	$6HDI + 4BzOH + Na^+ - 2CO_2 + 2H_2O$	50	V	4

[a] The calculated $\langle f_{NCO}\rangle_1$ and $\langle f_{NCO}\rangle_2$ averages were equal to 3.50 and 3.60, respectively.

polyols was calculated from the OH-number and molecular weights determined by VPO. The values of the number-average functionality $\langle f_{OH}\rangle_1$ for a particular set of samples of PCLD1250, PCLT900, PCLT300, and 4-f STAR, were equal, respectively to 1.87, 2.95, 2.87, and 3.99. For the PCLD, it was assumed that it contains mono alcohol as admixture, and the triols contain some diol (these distributions were used as input to calculations). This assumption gave the following value of the second-moment functionality average $\langle f_{OH}\rangle_2$ = 1.93, 2.97, 2.93, and 4.0, respectively.

$$\langle f_X\rangle_1 = \sum_{f_X} f_X n_f, \quad \langle f_X\rangle_2 = \frac{\sum_{f_X} {f_X}^2 n_f}{\sum_{f_X} f_X n_f} \qquad (1)$$

Here n_f is the number fraction of molecules having f_X functional groups X.

Triisocyanates Precursors−Determination of Their Functionality Distributions. The isocyanate component for model network preparation was a star−shaped cyclotrimer (Scheme 1d) of 1,6-diisocyanatohexane which contains higher oligomers and possibly a certain quantity of products from the reaction with residual water−molecules containing urea and biuret groups. Desmodur N3600 has narrower distribution than Desmodur N3300. The composition of the commercial samples varies somewhat from lot to lot depending on the production time and storage conditions of the samples. For determination of functionality distribution, the isocyanate groups were blocked with 1-pentanol and/or benzyl alcohol in slight excess (10%) at room temperature under catalysis with dibutyltin dilaurate (1000 ppm) for 2 days. The mass distribution was determined by electrospray ionization FT mass spectrometry (ESI−FT−MS) or MALDI−TOF−FT−MS. The method was similar to that used in ref 31. In Table 1 there are shown, as an example, results of composition distribution for a sample of Desmodur N3300 exhibiting the widest distribution of the components among samples used in this study.

The values of $\langle f_{NCO}\rangle_1$ and $\langle f_{NCO}\rangle_2$ for samples of Desmodur N3300 varied over several years from 3.5 and 3.6, respectively, to 3.3 and 3.4. For Desmodur N3600, $\langle f_{NCO}\rangle_1$ and $\langle f_{NCO}\rangle_2$ vary around 3.20 and 3.25, respectively. More details on functionality distributions can be found in ref 32.

The content of isocyanate groups obtained by summing the components (Scheme 2) was equal within experimental error to the content of NCO groups determined by the reaction with excess of di-*n*-butylamine (solution of 0.2 mol/L in dry THF) at room temperature to form substituted urea. The excess amine was then determined by potentiometric titration with hydrochloric acid (0.1 mol/L).

Preparation of Networks. Hydroxy-functional precursors−4-f STAR, PCLD, and PCLTs of different molecular weight−were dissolved in suitable solvents to get 20−80 wt % solutions. Dibutyltin dilaurate (500 ppm related to reactants) as catalyst in 1% solution in MAK or diglyme and Desmodur N3300 or N3600 were added. Always, the mixtures were stirred approximately for 3 min. The initial molar ratio [NCO]/[OH] was kept equal to one. The solution was poured into a glass mold to make sheet (about 2 mm thick). The samples were kept at room temperature for about 2 days, and later at elevated temperature (50 °C) for 1 day to achieve full conversion of NCO groups. The absence of unreacted NCO groups was confirmed by FTIR ATR test (the content of NCO groups was below 1 wt %).

Monitoring of Reaction between OH and NCO groups−FTIR Measurements. The decrease of the concentration of NCO groups was determined by FTIR spectroscopy. The decrease in the intensities of the stretching band at 2273 cm^{-1} was monitored. The intensity of NCO group band was related to the intensity of the reference C−H stretching band at 2930 cm^{-1}, which remains practically constant during the reaction.

Scheme 2. Structures of Oligomers Found in the Isocyanate Component

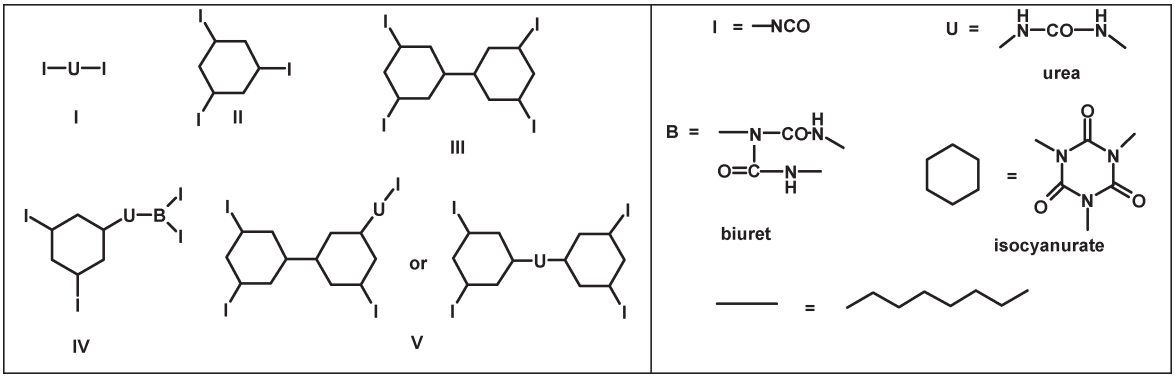

Gelation−Critical Time and Critical Conversion. The reactants, solvent and catalyst were mixed for about 3 min. Small portions of the material (approximately 0.5 g) were inserted into dried vials under inert gas and sealed. The vials were then kept in the temperature bath at 25 °C. Stepwise, at the several consequent reaction times when a substantial viscosity increase was observed as in ref 33, the solution of di-*n*-butylamine in THF was added to the reaction mixture in the vials and mechanically stirred. The secondary amine was used to quench the reaction by blocking of NCO groups. The amount of di-*n*-butylamine was always approximately 2-fold the molar content of NCO at the given conversion. The volume of THF was about 30 times larger than the volume of the polymerizing sample. A small amount of dichloromethane was added after a few seconds and mixed by shaking. Solubility was assessed by visual examination of the solution under mechanical agitation. The critical (gel) time was the first time at which insoluble fraction was registered. To validate the correctness and precision of the gel time determination, for several selected compositions of each system, a gel fraction determination was used in parallel. The gel fraction was determined as a function of reaction time and extrapolated to zero gel fraction. The gel times determined by the two methods gave the same result. In parallel, the conversion of NCO groups was determined by FTIR spectroscopy measuring a control sample of the same reaction mixture. The critical conversion was extrapolated at the gel-time from the both methods. The reproducibility of critical conversion was thus ±0.01 in conversion.

Determination of Swelling Degree. The pieces of crosslinked polymer of about 0.1−0.2 g were precisely weighed and put in a solvent the volume of which was about 50 times larger. Samples were temperature conditioned prior to their weighing (25 °C). After the full swelling, the solvent was exchanged several times to facilitate sol extraction. Samples were extracted until their weights at test temperature reached constant values. The fractions of sol were determined from the difference of dry samples before and after extraction. The volume fraction of polymer in the swollen sample (ϕ_2) was calculated from weights of the swollen sample (m_{sw}) and dry sample after extraction ($m_{pol} = m_{sw} - m_{solv}$) and specific gravities of the polymer (ρ_{pol}) and solvent (ρ_{solv})

$$\phi_2 = \frac{m_{pol}/\rho_{pol}}{m_{pol}/\rho_{pol} + (m_{sw} - m_{pol})/\rho_{solv}} \quad (2a)$$

The volume fraction of polymerizable material during network formation called "solids" is given by

$$\phi_2^0 = \frac{m_{pol}/\rho_{pol}}{m_{pol}/\rho_{pol} + m_{solv}^{nf}/\rho_{solv}} \quad (2b)$$

where m_{solv}^{nf} is the amount of solvent in the system at network formation.

Determination of Equilibrium Modulus and Dynamic Mechanical Measurements. Dynamic mechanical measurements (DMA) were performed using a dynamic mechanical analyzer Tritec 2000 (Triton Technology Ltd.). Rectangular samples (a free, unclamped specimen of length 5 mm, thickness from 1.5 to 3 mm, and width 10 mm), were used in fully clamped bending mode. Samples were measured in the equilibrium swollen state. In the swollen state, the frequency dependence of the complex Young modulus $E^* = E' + iE''$ (E' is storage and E'' loss modulus) was measured at ambient temperature. Frequency range from 0.1 to 30 Hz was used. Frequency measurements were done to be sure that at the given temperature the material is in the rubbery state. The swollen samples were measured in air atmosphere. The solvent content in the duration of measurement was considered constant as only less than 1% of the solvent evaporated during the test time. DMA of dry samples was performed using the same equipment. Temperature dependencies of the complex Young moduli were measured from −100 to +150 °C.

Results and Discussion

Critical (Gel-Point) Conversion. The gel-point conversion of NCO groups $(\alpha_{NCO})_{crit} \equiv \alpha_{crit}$ (all systems were stoichiometric), was determined by checking for full solubility of the reacting system (sometimes combined with extrapolation of the gel fraction to zero). The conversion of NCO groups was determined by FTIR or by reaction with dibutylamine.[9,10] The magnitude of dilution was characterized by the initial concentration of reactive groups c_0 (mol/cm^3) (includes both NCO and OH groups) or volume fraction of polymerizable components ϕ_2^0, where $\phi_2^0 = c_0/(c_0)_{bulk}$. The extrapolation of α_{crit} to $(1/c_0) \rightarrow 0$ or $1/\phi_2^0 \rightarrow 0$ should be equal to the critical conversion for the ring-free case, a quantity which can be calculated from the branching theory assuming all bonds are intermolecular (cf. also refs 24, 25, 34, and 35). The extrapolation extends over the nonexisting range of concentrations of functional groups higher than the concentration in undiluted (bulk) state for which $\phi_2^0 = 1$. The conversion of functional groups α is a sum of conversions to intermolecular and intramolecular bonds

$$\alpha = \alpha_{inter} + \alpha_{intra} \quad (3)$$

The question arises whether the dependence of α_{crit} on $1/\phi_2^0$ is linear as usually assumed. For bimolecular reactions, the rate of conversion of functional groups into intermolecular

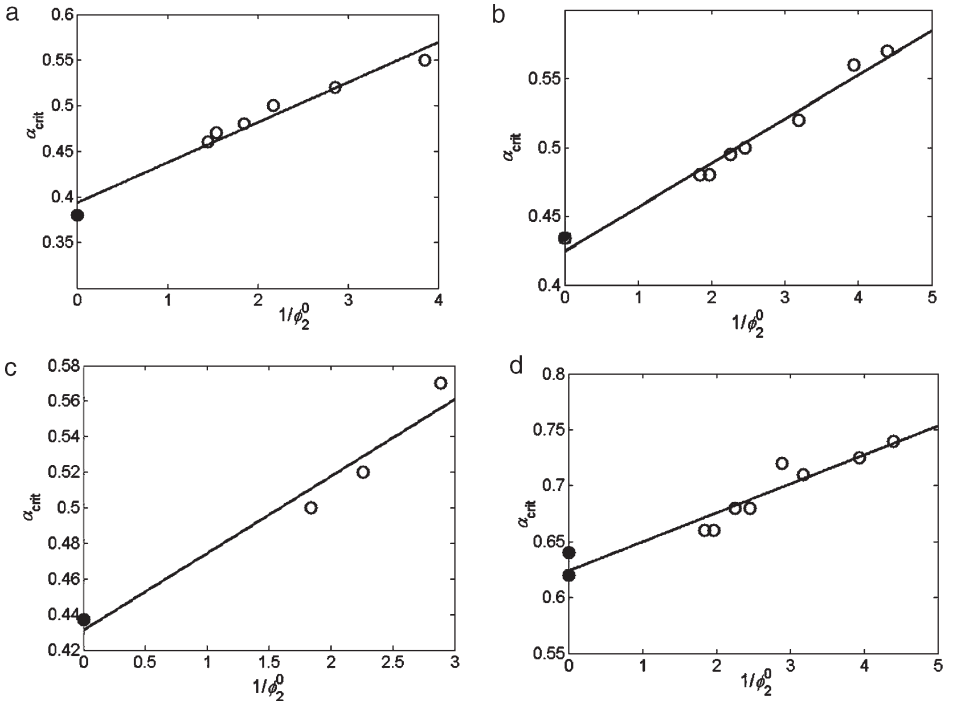

Figure 3. Gel-point conversion, α_{crit}, of polyols differing by functionality and molecular weight with a trimer of 1,6-diisocyanatohexane, Desmodur N3300, and Desmodur N3600, at 25 °C. Filled circles are theoretical ring-free values. Open circles experimental data. (a) 4-f STAR with Desmodur N3300; diluent methyl amyl ketone. (b) PCLT900 with Desmodur N3300; diluents methyl amyl ketone and diglyme. (c) PCLT300 with Desmodur N3300; diluent methyl amyl ketone. (d) PCLD1250 with Desmodur N3300 and/or N3600; diluents methyl amyl ketone and/or diglyme.

bonds is equal to

$$c_0 \frac{d\alpha_{inter}}{dt} = k_{inter} {c_0}^2 x_{NCO} x_{OH} \quad (4)$$

and the rate of formation of intramolecular bonds closing cycles reads

$$c_0 \frac{d\alpha_{intra}}{dt} = k_{intra} c_0 x_{NCO} x_{OH} \quad (5)$$

where x_{NCO} and x_{OH} are molar fractions of NCO and OH groups, respectively. From these two equations, it follows that

$$\frac{d\alpha_{intra}}{d\alpha_{inter}} = \frac{k_{intra}}{k_{inter}} \frac{1}{c_0} \quad (6)$$

If k_{intra} and k_{inter} are constant, we get for the gel-point conversion α_{crit}

$$\alpha_{crit} = (\alpha_{inter})_{crit} \left(1 + \frac{1}{c_0} \frac{k_{intra}}{k_{inter}}\right) \quad (7)$$

i.e., α_{crit} is a linear function of $1/c_0$. However, k_{intra} expressing all possibilities of closing cycles is somewhat dependent on conversion (it increases initially, because the number of opportunities of closing cycle increases). At higher degrees of cyclization (formation of compact structures), both k_{intra} and k_{inter} can decrease. Experimental experience shows that the $1/c_0$ dependence is fulfilled within experimental error ($\pm 1-2\%$) in most cases.[3] Unpublished results based on our new spanning-tree model with kinetically controlled bond formation probabilities show that the dependence of α_{crit} on $1/c_0$ is not exactly a straight line but the curvature is very small, so that linearization of plot α_{crit} vs $1/c_0$ is a good approximation (cf. also. ref 25).

The dependence of the critical conversion on dilution for the four precursors is shown in Figure 3,parts a−d. The ring-free value for $1/c_0 \rightarrow 0$ has been obtained by the statistical branching theory explained in the Appendix. Assuming the same reactivity, respectively, for NCO and OH groups of the precursors, the critical conversion for gelation is equal to eqs A-10 and A-11 of the Appendix

$${\alpha_{crit}}^2 = [(f_{OH} - 1)(\langle f_{NCO} \rangle_2 - 1)]^{-1} \quad (8)$$

where $\langle f_{NCO} \rangle_2$ is the second-moment average functionality of the triisocyanate which was determined experimentally as described in the Experimental Section.

Although some of the plots show up signs of curvature, the deviations from linearity are within experimental error. As expected, the extent of cyclization increases with increasing functionality of the polyols and decreases with their arm length. This data shows a large dependence of the fraction of intramolecular bonds on functionality and network chains length. Figure 4 shows the fraction of bonds lost in closing of cycles for cross-linking in systems containing 40 wt % diluent. This concentration was chosen because it is the working concentration for the tetrafunctional star when used in coatings. Within experimental error, no difference was found when diglyme and methyl amyl ketone (a somewhat poorer solvent) were used as diluents. Up to the gel point, the reaction products were quite soluble in both diluents. In this communication, the data of Figure 3, parts a−d, serve mainly for correlation of pregel and postgel cyclization.

Swelling and Phase State of Networks Prepared in the Presence of Diluents. Figure 5 shows the equilibrium degree of swelling in diglyme in dependence on dilution. The swelling degree increases with increasing dilution as expected, but (except of the PCLD1250 network) one or two samples of the highest dilutions take up in equilibrium (in contact with an excess of diluent) less diluent than was the volume of diluent

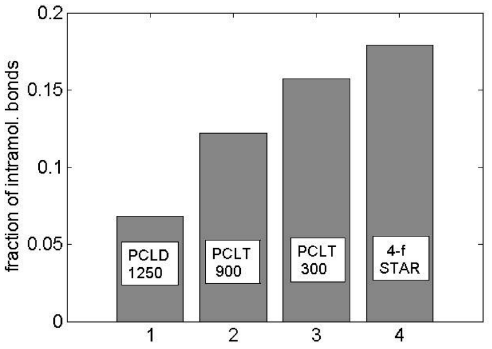

Figure 4. Fraction of intramolecular bonds of all bonds formed at the gel point for different precursors prepared in the presence of 40 wt % diluent (60 wt % solids).

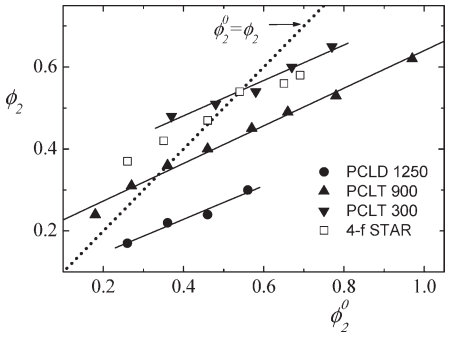

Figure 5. Equilibrium degree of swelling of networks in diglyme at 25 °C, expressed as volume fraction of polymer, ϕ_2, in dependence on dilution with diglyme during network formation, expressed as volume fraction of solids, ϕ_2^0.

during network formation (Figure 5). This indicates phase separation during network formation − expulsion of a part of solvent out of the sample at higher conversions. Indeed such a phenomenon was observed visually and it was a subject of consideration in conjunction with coating film formation.[36] Phase separation affects the memory factor and thus the values of concentration of EANCs calculated from equilibrium modulus. It is a subject of the following reasoning in this section.

Phase Separation. During cross-linking in the presence of diluent, phase separation can set in before, at or after the gel point. Before the gel point, phase separation starts when the formed branched polymer becomes incompatible with the diluent present in the system. After the gel point, it can happen when the cross-link density and possibly the associated changes of polymer segment−solvent interactions are such that the gel cannot absorb the amount of the diluent added at the beginning of the process. The key role is played by the memory term, ϕ_2^0. To clear its role and its changes during network formation, let us recall some basic thermodynamic relations. We will be examining the changes illustrated by the Scheme 3.

The phase equilibrium is determined by the equality of chemical potentials of components ($i = 1, 2, ...$) in coexisting phases (I, II, ...) $\mu_i^{\mathrm{I}} = \mu_i^{\mathrm{II}} = ...$ The change of Gibbs energy resulting from swelling is usually considered to be a sum of mixing and deformation of the network

$$\Delta G_{\mathrm{sw}} = \Delta G_{\mathrm{mix}} + \Delta G_{\mathrm{net}} \tag{9}$$

Let us first examine the network term because it is the memory factor ϕ_2^0 through which the memory of network history comes in (memory of shape). For a network of

Scheme 3. Cross-Linking of a System with Diluent Undergoing Phase Separation after the Gel Point

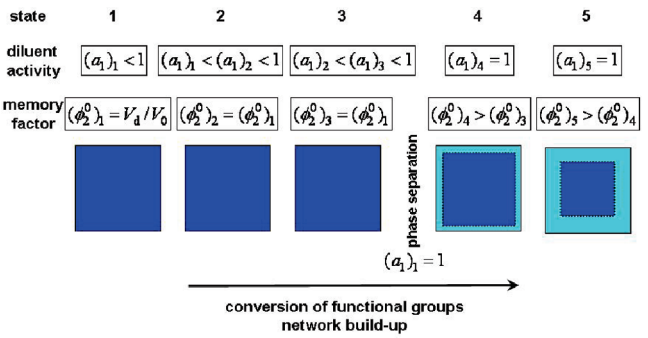

Gaussian chains in nearly Θ-solvent, it holds that[4,37]

$$\Delta G_{\mathrm{net}} = kTA(N_\nu/2)(\lambda_x{}^2 + \lambda_y^2 + \lambda_z{}^2 - 3) - B \ln \lambda_x\lambda_y\lambda_z \tag{10}$$

where k is the Boltzmann constant, T is the temperature in K, N_ν is the number of elastically active network chains, A, and B are factors in the Flory−Erman rubber elasticity theory depending on interchain interactions ($A = (f_e - 2)/f_e$, $B = 0$ for phantom networks, and $A = 1$, $B = 2/f_e$ for affine network), f_e is average number of EANCs issuing from elastically active junctions, cf., ref.;[38] $\lambda_x,\lambda_y,\lambda_z$ are deformation ratios, $\lambda_i = \langle r_i^2\rangle^{1/2}/\langle r_{i,\mathrm{ref}}^2\rangle^{1/2} \cong \langle r_i^2\rangle^{1/2}/\langle r_{i,\mathrm{nf}}^2\rangle^{1/2}$ and $\langle r_i^2\rangle^{1/2}$, $\langle r_{i,\mathrm{ref}}^2\rangle^{1/2}$,$\langle r_{i,\mathrm{nf}}^2\rangle^{1/2}$ are, respectively, the root-mean-square dimensions of chains in actual state, reference state (state of ease), and at network formation in the direction x, y, z. Passing to the chemical potential of the diluent, $i = 1$, $(\partial G_{\mathrm{sw}}/\partial N_1)_{Ni(i\neq 1)} = \Delta\mu_1$, spherical symmetry conditions are introduced. Let us further assume that the effect of addition of diluent is mainly its diluting effect, i.e., $V^{1/3} \propto \langle r^2\rangle^{1/2}$, $V_{\mathrm{nf}}{}^{1/3} \propto \langle r_{\mathrm{nf}}^2\rangle^{1/2}$ where V is system volume. Then

$$(\Delta\mu_1)_{\mathrm{net}}/RT = \nu_{e,\mathrm{nf}} V_{\mathrm{m1}} (A\phi_{\mathrm{rel}}{}^{-1/3} - B\phi_{\mathrm{rel}}) \tag{11}$$

where R is the gas constant, V_{m1} is the molar volume of the diluent, and

$$\phi_{\mathrm{rel}} = V_{\mathrm{nf}}/V \tag{12}$$

is the inverse *relative volume degree of swelling*, or volume fraction of polymer + added diluent in the swollen gel; $\nu_{e,\mathrm{nf}} = (N_\nu/N_{\mathrm{Avogadro}})/V_{\mathrm{nf}}$ is now the concentration of EANCs in moles per volume of the polymer + diluent mixture. For $\phi_{\mathrm{rel}} = 1$, and for the Flory−Erman junction fluctuation theory, this equation simplifies further

$$(\Delta\mu_1)_{\mathrm{net}}/RT = \nu_{e,\mathrm{nf}} V_{\mathrm{m1}} (A - B) = \nu_{e,\mathrm{nf}} V_{\mathrm{m1}} \frac{f_e - 2}{f_e} \tag{13}$$

which, in conjunction with the condition of equilibrium with pure diluent, $(\Delta\mu_1)_{\mathrm{sw}} = 0$, is the condition for phase separation. Thus, under these conditions the contribution to chemical potential of the forming network farther from the gel point (sol fraction →0, $f_e \to f_{\mathrm{chem}}$) does not depend on ϕ_{rel}, and the proportionality constant, $(f_e - 2)/f_e$, is the same *irrespective of whether the network is phantom or affine*. However, for swelling measurements the use of $\nu_{e,\mathrm{nf}}$ is somewhat impractical; because the concentration of EANCs should not depend on the amount of diluent or extent of phase separation. The memory term is normally related to

the dry state

$$\phi_2^0 = V_{dry}/V_{nf} \tag{14}$$

Two options can be considered

$$V_{dry} = V_{sol} + V_{gel}(a) \quad \text{or} \quad V_{dry} = V_{gel}(b)$$

One uses definition (a) whenever one works at constant volume equal to the volume at network formation, where the network chains are at their state of ease, for instance, in the case of continuous rheology measurements or vapor pressure measurements during network formation. The concentration of EANCs is then expressed accordingly. According to definition (b), sol is taken as a part of the diluent. This definition should be used whenever measurements are performed with extracted samples. The concentration of EANCs is then related to the volume of gel. Important is that both definitions are the same farther from the gel point, when the amount of sol is much smaller than the fraction of gel and thus sol can be neglected. Thus, in the elastic contribution

$$\begin{aligned} \nu_{e,dry} \equiv \nu_e &= \nu_{e,nf}(V_{nf}/V_{dry}) = \nu_{e,nf}/\phi_2^0 \\ \phi_2 &= \phi_{rel}(V_{nf}/V_{dry}) = \phi_{rel}/\phi_2^0 \end{aligned} \tag{15}$$

Using the redefined quantities

$$(\Delta\mu_1)_{net}/RT = \nu_e V_{m1}[A{\phi_2}^{1/3}(\phi_2^0)^{2/3} - B\phi_2] \tag{16}$$

For $\phi_2 = \phi_2^0$ (cf., ref 39)

$$\begin{aligned} (\Delta\mu_1)_{net}/RT &= \nu_e V_{m1}\phi_2(A-B) \\ &= \nu_e V_{m1}\phi_2[(f_e-2)/f_e] \end{aligned} \tag{17}$$

For $(\Delta\mu_1)_{mix}$, one usually takes the Flory−Huggins equation[40] or Krigbaum and Carpenter version[41] for ternary system. Near the gel point or for off-stoichiometric system, the cross-linking system is composed of the diluent, the sol, and the gel. The sol itself is composed of a distribution of branched polymers. To make the situation simpler, the system has been considered as a pseudoternary system, the components being the diluent (component 1), the gel (2) and pseudomonodisperse sol as component 3[36] (cf. footnote 52).

In the experimental range of gels studied in this contribution, at the moment of phase separation the fraction of soluble molecules is small and $\phi_2 = \phi_2^0$ are constant, so that the condition for equilibrium with solvent vapors reduces to

$$\ln(1-\phi_2^0) + \phi_2^0 + \chi(\alpha)(\phi_2^0)^2 + V_{m1}\phi_2^0\nu_e(\alpha)(A-B) = \ln a_1 \tag{18}$$

Before phase separation, the volume is constant ($\phi_2 = \phi_2^0 =$ const) and $\nu_e(\alpha)$ and possibly $\chi(\alpha)$ depend on conversion of functional groups, α. Consequently, the activity of solvent a_1 changes (increases, Scheme 3). At the moment of phase separation $a_1 = 1$ (coexistence of saturated vapor with pure solvent), the conversion α reaches its critical value, α_{cs}, (subscript cs refers to critical with respect to phase separation) which determines the critical values of concentration of EANCs and of the interaction parameter

$$\ln(1-\phi_2^0) + \phi_2^0 + \chi(\alpha_{cs})(\phi_2^0)^2 + V_{m1}\phi_2^0\nu_e(\alpha_{cs})(A-B) = 0 \tag{19}$$

By increasing the conversion, more and more diluent separates: a_1 remains equal to 1, but the memory term ϕ_2^0 starts changing because the new EANCs are formed at their state of ease corresponding to a smaller volume, so that in the final dry network they are less compressed (Scheme 3). The product $\phi_{2sep}^0\nu_e(\alpha)$ (eq 21) is obtained by adding the contributions—a method conceptually related from the two-network hypothesis of Tobolsky et al.[42] The condition for swelling equilibrium with the diluent can be expressed as

$$\ln(1-\phi_2) + \phi_2 + \chi\phi_2^2 + V_{m1}A\nu_e[{\phi_2}^{1/3}(\phi_{2sep}^0)^{2/3} - B\phi_2] = 0 \tag{20}$$

where the quantities ϕ_2, χ, ν_e depend on conversion α and ϕ_{2sep}^0 depends on their changes with conversion. For conversions at $\alpha > \alpha_{cs}$, the memory term ϕ_{2sep}^0 is determined by the equation

$$\phi_{2sep}^0\nu_e(\alpha) = (\nu_e)_{cs}\phi_2^0 + \int_{(\nu_e)_{cs}}^{\nu_e(\alpha)} \phi_2(\alpha)\, d\nu_e \tag{21}$$

or

$$\phi_{2sep}^0\nu_e(\alpha) = (\nu_e)_{cs}\phi_2^0 + \int_{\alpha_{cs}}^{\alpha} \phi_2(\alpha)\frac{d\nu_e(\alpha)}{d\alpha}\, d\alpha \tag{22}$$

The values of ϕ_{2sep}^0 are then used for calculation of ν_e from the equilibrium modulus. The ϕ_{2sep}^0 values are obtained by solving the integral eqs 20, after substitution for ϕ_{2sep}^0 from eqs 21 or 22, numerically, for instance as difference equations. The interaction parameter also depends on conversion. This dependence was obtained from the equilibrium swelling degree and equilibrium modulus of samples prepared at different dilutions where phase separation did not occur. In our calculations, the dependence was expressed as a linear function of intermolecular conversion of functional groups, α_{inter}, calculated from the experimental concentration of EANCs and theoretical dependence of ν_e on α_{inter} (for details, see Appendix). This procedure was applied to modulus data analyzed in the next section. Beyond this point, these dependences are not further analyzed.

Equilibrium Modulus and Concentration of Elastically Active Network Chains (EANCs). The storage modulus, E', of swollen samples is practically independent of frequency in the range of frequencies 0.01−10 Hz which means that the values are free of relaxation effects. The decrease of the frequency independent storage modulus of swollen fully reacted samples is shown in Figure 6. The differences in the moduli correlate with equivalent weights per potential EANC; the decrease of E' is almost linear with ϕ_{2sep}^0. The modulus falls to zero at the limiting value of dilution for which the gel point is shifted to full conversion of functional groups[9] and beyond which a coherent gel ceases to form. For correlations, only experimental data on swollen samples were used but the values of E' for dry samples measured at their rubbery region at elevated temperatures are also displayed and will be briefly discussed later.

For the small-strain Young modulus after expansion of deformation function into power series of strain, the relationship E reads

$$E \cong E' = 3RTA\nu_e{\phi_2}^{1/3}(\phi_2^0)^{2/3} \tag{23}$$

For samples that underwent phase-separation during their preparation, ϕ_2^0 should be replaced by ϕ_{2sep}^0(cf., eqs 21, 22).

Equation 23 has been used for calculation of the concentration of elastically active network chains (EANC) in moles per volume of dry sample. The dependence on ϕ_2^0 is shown in Figure 7a−d.

For the samples where phase separation took place and ϕ_2^0 was replaced by ϕ_{2sep}^0, the values of ν_e are also somewhat different. The largest difference was found for the network of 4-f STAR. After correction, the dependence smoothly proceeds to the limiting dilution limit at which coherent gels cease to be formed. We are not able to say what happens in the region of very weak gels, somewhere below $\nu_e = 10^{-4}$ mol/cm^3, because the gels are too weak for determination of modulus.

To find out whether interchain interactions can have an effect on equilibrium modulus, we investigated also dry networks at elevated temperatures (80 °C). Usually, the values of ν_e for dry networks are somewhat higher than those obtained from measurements of swollen samples due to stronger interchain interactions in denser system. Surprisingly, some of the ν_e-values obtained by measurements in the dry state (after recalculation of ν_e to 25 °C) were lower than those in the swollen state. However, the ν_e-values for swollen and dry samples close to the phase separation limit were practically the same. More cross-linked/less diluted samples that took up in equilibrium more additional solvent showed up this deviation. The decrease in ν_e was about 15% which slightly exceeds experimental error. We think that such deviation can be caused by commencing effect of finite extensibility of network chains in the swollen networks: the network chains are considerably shorter than in typical soft rubbers.

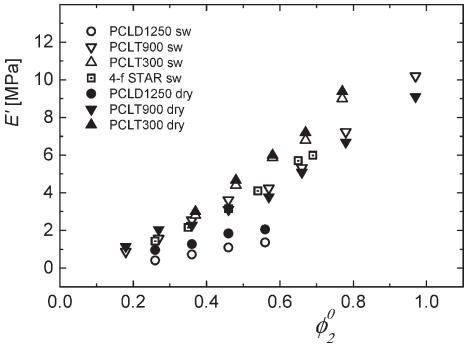

Figure 6. Storage moduli of swollen and dry samples of networks made of various OH precursors and trimer of 1,6-diisocyanatohexane (triisocyanate) as a function of dilution at network preparation expressed as volume fraction of solids, ϕ_2^0. Testing of swollen samples performed at 25 °C, dry samples tested above their T_g; networks containing PCLD 1250 were tested at 35 °C, PCLT300 at 80 °C, and PCLT 900 at 27 °C.

Lowering of equilibrium modulus, which correlated with decrease of concentration of elastically active network chains (EANC), was the main objective of investigations on mechanical properties, however the dilution effect on some other properties of dry networks was also studied. With increasing dilution at network preparation, the maximum of the loss angle tangent (tan δ), T_{max}, corresponding to the glass transition is somewhat shifted to lower temperatures and the transition gets broader. The shift of the maxima does not exceed 6 K when moving from $\phi_2^0 = 1$ to $\phi_2^0 = 0.2$. Since the number of bonds is the same for all samples (conversion of functional groups is close to 100%), it is only the cross-link density which is different, and it has a secondary effect. Also the width of the transition increases with increasing dilution due to the shift to the assumed blob structure of the highly diluted networks.[9]

Scaling Relations. Scaling of equilibrium modulus and degree of swelling against ϕ_2^0 has been a subject of numerous papers. Theoretical analysis by Rubinstein, Colby, and Obukhov[43,44] and experimental examination by Cohen[45] can be taken as representative examples. For the four series

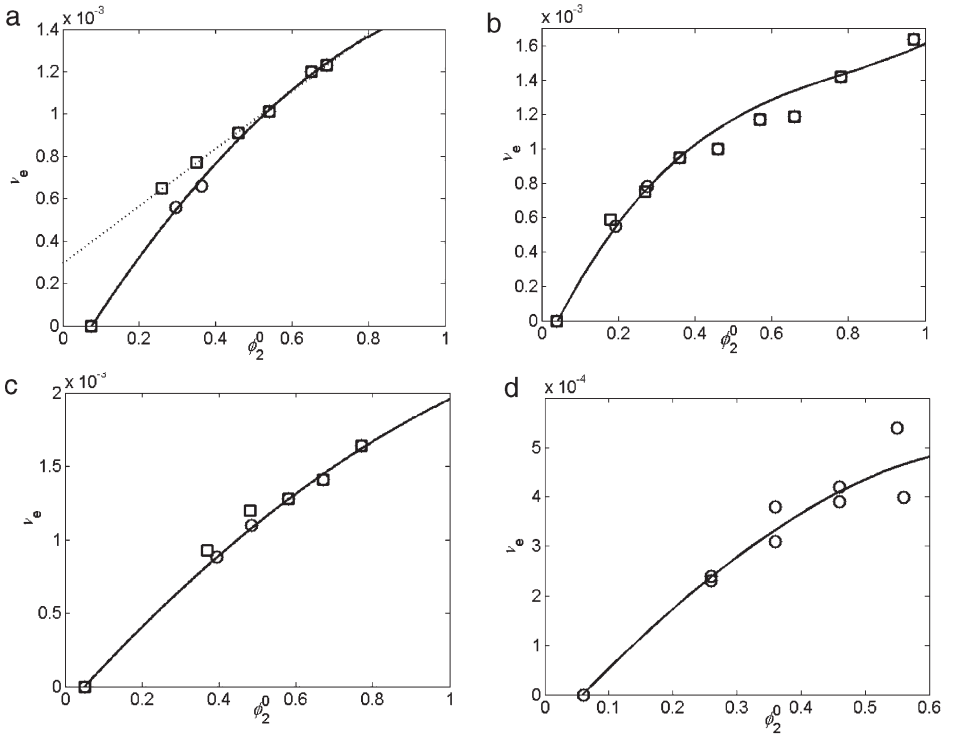

Figure 7. (a−d) Concentration of EANCs as a function of volume fraction of solids. Squares; ϕ_2^0 not considering phase separation. Circles: effect of phase separation on ϕ_2^0 respected (ϕ_{2sep}^0 used); full lines: interpolation. Key: (a) 4-f STAR network; (b) PCLT900 network; (c) PCLT300 network; (d) PCLD1250 network.

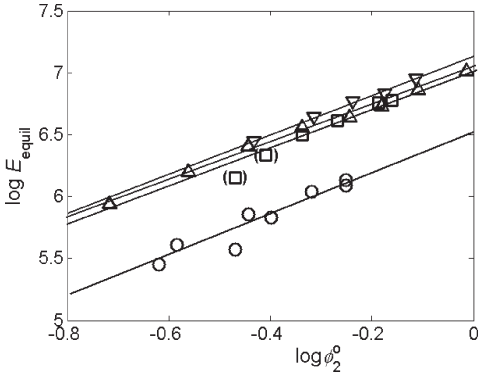

Figure 8. Scaling of Young modulus of equilibrium swollen gels in diglyme vs volume fraction of solids at network formation at 25 °C; series of networks: (□) 4-f STAR; (△) PCLT900; (▽) PCLT300; (○) PCLD1250; ((□)) data points of phase-separated samples not taken into account.

of samples discussed here, the log−log plots of E' vs. ϕ_2^0 (Figure 8) and ϕ_2 vs. ϕ_2^0 are pretty linear if the phase-separated samples are excluded. For the scaling relations

$$E' \propto (\phi_2^0)^x \tag{24}$$

and

$$\phi_2 \propto (\phi_2^0)^y \tag{25}$$

the values of exponents were found to be

$$x = 1.77 \quad \text{and} \quad y = 0.54$$

The scatter of the values of exponent x for individual series is illustrated by the series 1.88, 1.75, 1.69, 1.75 for 4-f STAR, PCLT900, PCLT300, and PCLD1250 (mean value 1.77); the same series for y reads 0.53, 0.54, 0.55, (0.70). The scaling dependence E vs. ϕ_2^0 is shown in Figure 8.

Sivasailam and Cohen[46] found for PDMS networks diluted by nonfunctional PDMS that the exponents x varied with lengths of EANCs from $x = 2.07$ for EANCs of $M_n = 10^5$ to $x = 1.52$ for EANCs of $M_n = 10^4$. Our systems, of relatively high cross-link density where entanglements do not play any important role, are closer to those corresponding to the lower limit of M_n. Also for PDMS networks,[41] the exponent y falls from 0.65 to 0.50 which is close to our value of 0.54. In this plot (E *vs.* ϕ_2^0), the dependences do not fit the limiting dilution data point ($E = 0$ for $\phi_2^0 = \phi_{2\text{lim}}^0$) and they must be curved downward with progressive dilution, i.e., the exponent x would grow over the value 2 as predicted in refs 43 and 44 if the systems would not phase separate. For systems of higher potential cross-link density, nanogel formations are formed at high dilutions first and they are in the later stages chemically connected and form a macrogel−a mechanism so well documented for chain cross-linking (co)polymerization.[11−15]

Using the experimental values of exponents $x = 1.77$ and $y = 0.54$ in combination with eq 23 one can deduce how the concentration of EANCs, ν_e, scales with ϕ_2^0

$$\nu_e \propto (\phi_2^0)^z \tag{26}$$

The value of z was found to be 0.92 which is in absolute value close to the scaling factor $(\phi_2^0)^{-1}$ satisfying the shift of the gel point conversion. This is a good promise for a simple correlation between the increase of critical conversion and lowering of the equilibrium modulus. Colby and Rubinstein[46] predicted for the exponent z the value $^4/_3$ for Θ-solvents, but their reasoning was based on disentanglement by dilution which is limited to the family of gels with long chains having very low number of cross-linkable sites. Such a case does not apply here.

Interrelation between Pregel Cyclization and Lowering of the Modulus. In this section, we will test the ansatz that pregel cyclization can be correlated with the formation of the elastically inactive cycles in the network and that the decrease of modulus by dilution can be translated into a decrease of intermolecular conversion, α_{inter} (the experimental conversion was close to 100%). The values of α_{inter} were obtained from experimental values of ν_e (calculated from equilibrium modulus) using the theoretical dependence of ν_e on α_{inter} derived by the branching theory (see Appendix).

The meaning of terms of (effectively) "intermolecular" and "intramolecular" conversion used here needs a clarification. Beyond the gel point all gel−gel reactions are essentially intramolecular (they occur between groups attached to the gel "molecule"). If all strands between cross-links are considered elastically active (EANCs), their number is equal to the cycle rank of the network (ref 4) which can be easily calculated for a perfect network. The *effective* cycle rank is lower than the ideal value, possibly due to incompleteness of the reaction or off-stoichiometry, but also due to formation of *elastically inactive cycles* within the network, existing also in fully reacted systems. These cycles do not contribute to the (elastically) effective cycle rank. The "ring-free" branching theory generates the effective cycle rank beyond the gel point under the premise that chains of all closed circuits are elastically active. In reality, their actual number, at the given conversion, (sensed, e.g., by equilibrium modulus) is lower. The difference is assigned to the formation of effectively intramolecular bonds. The conversion necessary for reaching the actual cycle rank (modulus) in the absence of elastically inactive cycles is called effectively intermolecular.

The following results were obtained.

In the difference $\Delta\alpha_{crit} = 1 - \alpha_{crit}$, α_{crit} is the experimentally determined critical gel-point conversion and for $\alpha_{crit} = 1$, $\nu_e = 0$. Also, $\nu_e = 0$ when $\alpha_{inter} = (\alpha_{crit})_{rf}$; $(\alpha_{crit})_{rf}$ is the ring-free value of gel-point conversion which has been calculated from the branching theory. This value is within experimental error equal to that obtained by extrapolation of α_{crit} to $1/\phi_2^0 \rightarrow 0$ (cf., Figure 3). One can see that a linear correlation of the shift of the gel point and lowering of modulus exists, cf., Figure 9. The slopes vary around unity (0.7, 1.0, 1.1, 1.2).

The question remains, how to use these interrelations for estimation of the decrease of the concentration of EANCs. It is worthwhile to use reduced quantities: The theoretical dependence of ν_e on α_{inter} starts at $(\alpha_{inter})_{crit}$ and ends at $\alpha_{inter} = 1$ and the values of ν_e depend on components functionality and equivalent weights per functional group etc. Therefore, the relative theoretical concentration of EANCs defined as

$$(\nu_e)_{rel} = \nu_e(\text{theor})/\nu_{e,\,max}(\text{theor}) \tag{27a}$$

was used, where $\nu_{e,max}$ is the maximum value of ν_e for $\alpha_{inter} = 1$. For the concentration of EANCs, $(\nu_e)_{rel}$ was plotted against

$$\Delta = \frac{\alpha_{inter} - (\alpha_{inter})_{crit}}{1 - (\alpha_{inter})_{crit}} \tag{27b}$$

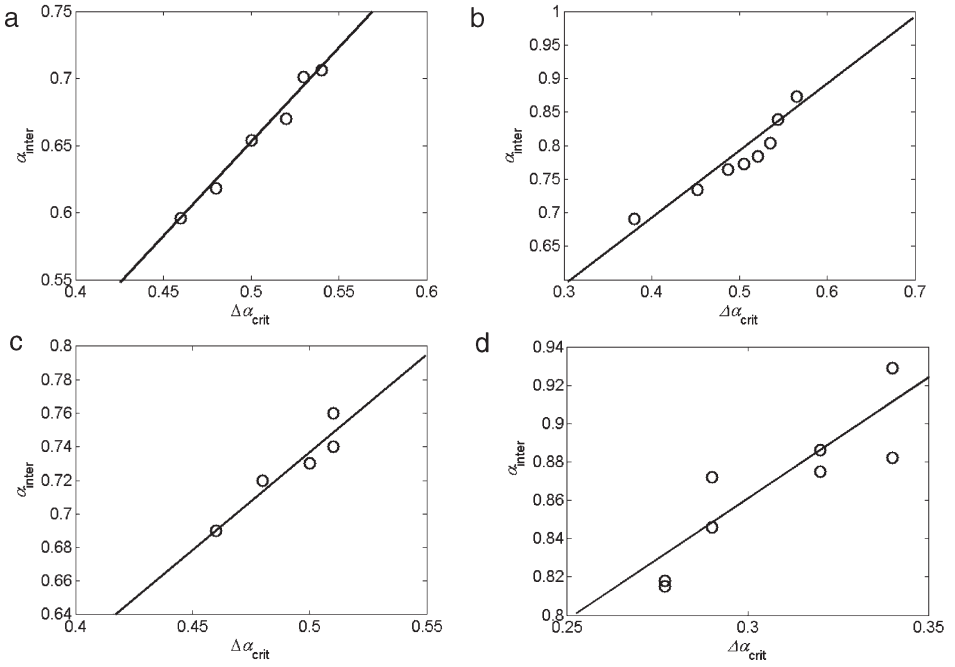

Figure 9. (a−d) Dependence of intermolecular conversion of functional groups on $\Delta\alpha_{crit} = 1 - \alpha_{crit}$. Key: (a) 4-f STAR networks; (b) PCLT900 networks; (c) PCLT300 networks; (d) PCLD1250 networks.

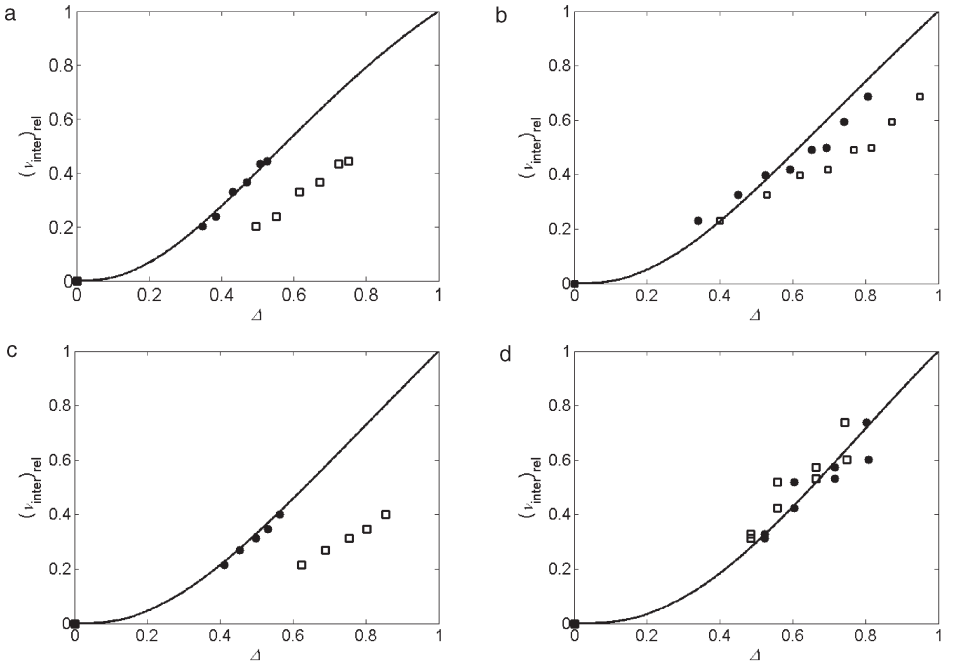

Figure 10. (a−d) Theoretical dependence of $(\nu_{inter})_{rel}$ on $\Delta = (\alpha_{inter} - (\alpha_{inter})_{crit})/(1 - (\alpha_{inter})_{crit})$, and experimental dependence of $(\nu_{inter})_{rel}$ on $\Delta = (1-\alpha_{crit})(\phi_2^0)^{1/3}/(1 - (\alpha_{inter})_{crit})$. Key: squares, primary data; full circles, data after applying the superposition factor; (a) 4-f STAR network; (b) PCLT900 network; (c) PCLT300 network; (d) PCLD1250 network.

These plots are independent of dilution since all reactions are considered intermolecular, α_{inter}.

The second set of data, comprise experimental concentrations of EANCs obtained from equilibrium modulus also reduced by dividing with the theoretical maximum value

$$(\nu_e)_{rel} = \nu_e(exp)/\nu_{e,max}(theor) \qquad (27c)$$

The abscissa reflects a relative change in critical conversion. The reference is the limiting dilution at which $\nu_e = 0$, when $\alpha_{crit} = 1$. Therefore, the abscissa variable should be $1 - \alpha_{crit}$ which is then reduced by the maximum available range of conversions where gel can exist:

$1-(\alpha_{inter})_{crit}$. We found that good fits were obtained when this quantity was multiplied by $(\phi_2^0)^{1/3}$. Thus, $(\nu_e)_{rel}$ was plotted against

$$\Delta = \frac{1-\alpha_{crit}}{1-(\alpha_{inter})_{crit}}(\phi_2^0)^{1/3} \qquad (27d)$$

These two dependences in log−log plots run parallel each other and can be superimposed by a horizontal shift. For

linear plot, superposition can be achieved by a multiplication factor (superposition factor, f_{sup}) – a constant for each set of networks. This superposition is shown in Figures 10; the values of f_{sup} are equal to 0.70, 0.85, 0.66, and 1.08, respectively, for networks of 4-f STAR, PCLT900, PCLT300, and PCLTD1250. This means that f_{sup} increases with the molecular mass of the precursor.

The figures also show the utilization of the maximum cross-link capacity of the systems. Normally, the highest concentration of EANCs is associated with the networks obtained without diluent (bulk systems). However in such networks a part of bonds is wasted in elastically inactive cycles. If cyclization were suppressed, we could reach the cross-link density corresponding to $\alpha_{inter} = 1$. The figures show that the utilization of the maximum cross-link capacity of samples presented here is only about 50% or less for 4-f STAR and PCLT300 networks and 70–80% for networks of PCLT900 and PCLD1250. The "unused" capacity is due to the fact that some samples were not or could not be prepared without diluent - the maximum ϕ_2^0 in our series was 0.7, 1.0, 0.8, and 0.7, respectively, for 4-f STAR, PCLT900, PCLT300, and PCLD1250. The remaining part is due to bonds wasted in closing elastically inactive cycles in networks formed in the absence of diluent. That remaining part could be potentially utilized if, for instance, the structure changed and the network chains were less prone to closing cycles.

What are the practical implications of this correlation? Can one get a good estimate of lowering of concentration of EANCs and modulus from experimental measurements of the shift of critical conversion? One needs at least one value of the experimental shift of critical conversion by dilution and one value of equilibrium modulus for a network prepared at the same dilution. Then, concentrations at other dilutions can be estimated. The procedure consists of four steps; it is visualized in Figure 11 showing the sequence of steps to be done:

1. The black curve—the dependence of $(\nu_e)_{rel}$ (eq 27c)—is calculated as explained in the Appendix. Also, the critical conversion of the ring-free system is calculated
2. For selected dilution given by ϕ_2^0 the critical conversion is determined experimentaly. Also, for the same dilution the equilibrium modulus is determined and $(\nu_e)_{rel}$(exp.) is calculated. The experimental data, $(\nu_e)_{rel} - \Delta$ (eq 27d) is given by the red circle.
3. The horizontal distance to the black curve gives the length b; from this f_{sup} is calculated.
4. The values of the black curve are multiplied by the superposition factor f_{sup}, which gives the red curve. The red curve serves for reading off values of $(\nu_e)_{rel}$ for other values of ϕ_2^0 . Linear dependence between the reference critical conversion and ring-free critical conversion as a function of $1/\phi_2^0$ is assumed

Conclusions

Several polyurethane networks were prepared from star-shaped precursors in the presence of varying amount of diluent. The shift of the gel point to higher conversions of functional groups, decrease of equilibrium modulus, and increase of equilibrium degree of swelling with increasing dilution were determined. The percentage of bonds wasted in cycles at the gel point increases with increasing functionality of the precursors and with their decreasing molecular mass. This conclusion also applies to the equilibrium modulus of networks with fully reacted functional groups. Some of the samples containing more diluent

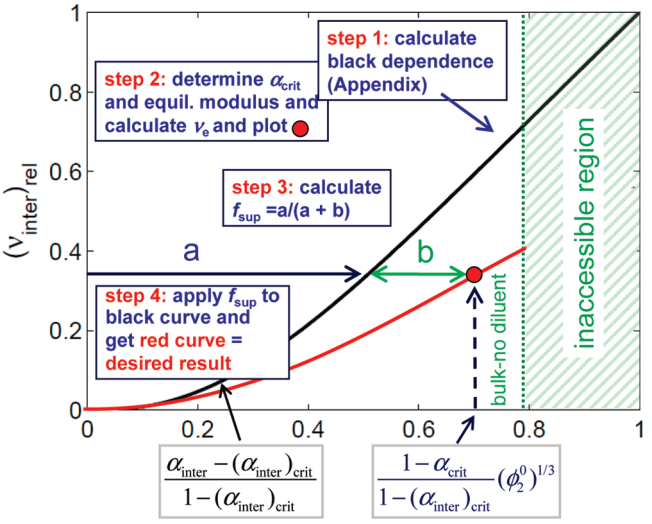

Figure 11. Sketch showing the procedure for estimation of the dependence of concentration of EANCs on dilution from the effect of dilution on the critical gel-point conversion ($f_{sup} < 1$).

showed up phase separation occurring during network formation in the form of macrosyneresis as a consequence of too high cross-link density. For such samples, the memory term ϕ_2^0 is larger than the initial volume fraction of solids because the newly formed elastically active network chains are formed in a volume which is smaller than that before phase separation. This fact must be respected when the concentration of EANCs is calculated from equilibrium modulus or equilibrium degree of swelling. Scaling relations between equilibrium modulus and degree of dilution are characteristic of systems in which entanglement contribution is unimportant; approaching the limiting dilution, the mechanism of network build-up changes and becomes dominated by hindered reactivity of groups in nanogel formations. For moderately diluted systems without phase separation, a correlation was found between the shifts of the gel point and lowering of the concentration of EANCs resulting from dilution during network formation and a method was proposed to estimate the concentration of EANCs from gelation measurements. The branching theory of a ring-free system is the clue of this correlation.

Acknowledgment. The authors acknowledge for the support of this work the Grant Agency of the Czech Republic (GACR 106/08/1409), the EU Framework Programme NANOPOLY (PITN-GA-2009-238700) and the financial support of the Ministry of Education, Youths, and Sports of the Czech Republic (MSM 0021620835).

Appendix

Derivation of Conditions for Gelation and Relations for Network Parameters. The statistical treatment of the network build-up is based on the theory of branching processes. Examples of application to similar systems can be found elsewhere.[47–51]

The basic distribution of building units is described by the following probability distribution function

$$F_{0n}(\mathbf{Z},\mathbf{z}) = n_A Z_A^{M_A}(1-\alpha_A+\alpha_A z_{AB})^{f_A} + n_B \sum_j x_j Z_B^{M_{Bj}}(1-\alpha_B+\alpha_{BA} z_{BA})^{f_{Bj}} \quad \text{(A-1)}$$

where

$$n_A = 1 - n_B \sum_j x_j = 1$$

Balance equations and definitions:

It holds that

$$n_A f_A \alpha_A = n_B \alpha_B \sum_j x_j f_{Bj} = n_B \alpha_B \langle f_B \rangle_n \quad \text{(A-2)}$$

The initial ratio of A to B groups, r_A, determines n_A and n_B

$$r_A = \frac{n_A f_A}{n_B \langle f_B \rangle_n}, \quad n_A = \frac{r_A \langle f_B \rangle_n}{r_A \langle f_B \rangle_n + f_A} \quad \text{(A-3)}$$

and

$$r_A \alpha_A = \alpha_B \quad \text{(A-4)}$$

The mass fractions of the components A and B, m_A and m_B, are given by

$$m_A = 1 - m_B = \frac{n_A M_A}{n_A M_A + n_B \sum_j x_j M_{Bj}} \quad \text{(A-5)}$$

Also, the number, n_{Bj}, and mass, m_{Bj}, fractions of B components in the whole system will be needed

$$n_{Bj} = n_B x_j m_{Bj} = \frac{n_{Bj} M_{Bj}}{n_A M_A + \sum_j n_{Bj} M_{Bj}} \quad \text{(A-6)}$$

For structure build-up, the pgfs, $F(\mathbf{Z},\mathbf{z})$ for the number of additional bonds issuing from units already bound by one of its bonds are needed. They are obtained from the pgf A-1 by differentiation with respect to z_{AB} and z_{BA}, respectively. The function F_{BA} describes the distribution of the $j-1$ ($1 \le j \le f_A$) of outgoing bonds A → B from a unit A already bonded by one incoming bond B → A

$$F_{BA}(Z_B, z_{AB}) = Z_A^{M_A}(1 - \alpha_A + \alpha_A z_{AB})^{f_A - 1} \quad \text{(A-7)}$$

Analogously

$$F_{AB}(Z_B, z_{BA}) = \sum_j x_j f_{Bj} Z_B^{M_{Bj}}(1 - \alpha_B + \alpha_B z_{BA})^{f_{Bj} - 1}/f_{Bn} \quad \text{(A-8)}$$

Equations A-7 and A-8 give access to molecular mass averages. In this work, we are not concerned with molecular mass averages, but only with the gel point and postgel properties. The mass-average molecular mass diverges at the gel point when the infinite structure appears in the system for the first time. The M_w diverges when the denominator $D = 0$. It can be shown that D is a function of the values of derivatives of F_{AB} and F_{BA}

$$D = 1 - F_{BA}^{AB} F_{AB}^{BA} = 0 \quad \text{(A-9)}$$

where

$$F_{BA}^{AB} = \left[\frac{\partial F_{BA}(Z_A, z_{AB})}{\partial z_{AB}}\right]_{Z_A = z_{AB} = 1},$$

$$F_{AB}^{BA} = \left[\frac{\partial F_{AB}(Z_B, z_{BA})}{\partial z_{BA}}\right]_{Z_B = z_{BA} = 1}$$

After substitution, condition A-9 reads

$$\alpha_A \alpha_B (f_A - 1)\left(\sum_j x_j f_{Bj}(f_{Bj} - 1)/\langle f_B \rangle_n\right) = \alpha_A \alpha_B (f_A - 1)\left(\sum_j x_j f_{Bj}^2/\langle f_B \rangle_n - 1\right) = 1 \quad \text{(A-10)}$$

or

$$\alpha_A \alpha_B (f_A - 1)(\langle f_B \rangle_2 - 1) = 1 \quad \text{(A-11)}$$

where

$$\langle f_B \rangle_2 = \sum_j x_j f_{Bj}^2 / \sum_j x_j f_{Bj} \quad \text{(A-12)}$$

is the second-moment functionality average (incorrectly called mass- or weight-functionality average because it has nothing to do with mass).

Equation A-11 is identical with the Stockmayer[47] expression for systems where all A−B bonds are formed with the same probability independent of the state of all other groups.

Postgel State. Various quantities characterizing the sol and gel in the postgel state can be calculated but we will restrict the calculation to sol fraction and concentration of elastically active network chains (EANCs) because this work is focused on changes of modulus of elasticity.

The quantities governing the postgel state are the extinction probabilities, v_{BA} and v_{AB}, derived from the pgfs F_{BA} and F_{AB}. They are equal to conditional probabilities, given that the respective bond exists, it has only a finite continuation:

$$v_{BA} = (1 - \alpha_A + \alpha_A v_{AB})^{f_A - 1} \quad \text{(A-13)}$$

$$v_{AB} = \sum_j x_j f_{Bj}(1 - \alpha_B + \alpha_B v_{BA})^{f_{Bj} - 1}/\langle f_B \rangle_n \quad \text{(A-14)}$$

The extinction probabilities are obtained by numerical solution of eqs A-13 and A-14. The extinction probabilities are roots in the interval ⟨0,1).

The mass fraction of sol is contributed by units issuing all bonds with only finite continuation. The units contribute by their mass (cf., eq A-6)

$$w_s = m_A(1 - \alpha_A + \alpha_A v_{AB})^{f_A} + \sum_j m_{Bj}(1 - \alpha_B + \alpha_{BA} z_A)^{f_{Bj}} \quad \text{(A-15)}$$

The concentration of EANCs is contributed by elastically active junctions, i.e., such units that participate at least in three bonds with infinite continuation. The pgf describing the states of units with respect to the number of issuing bonds with infinite continuation reads

$$\begin{aligned} T(z) &= n_A T_A(z) + n_B T_B(z) = \sum_{i=0} t_i z^i \\ T_A(z) &= (1 - \alpha_A + \alpha_A(v_{AB} + (1 - v_{AB})z))^{f_A} \\ T_B(z) &= \sum_j x_j (1 - \alpha_B + \alpha_{BA}(v_{BA} + (1 - v_{BA})z))^{f_{Bj}} \end{aligned} \quad \text{(A-16)}$$

Each bond with infinite continuation contributes by 1/2 to the number of EANCs, N_e. Thus,

$$N_e = (1/2) \sum_{i=3}^{f_A, f_B} i t_i \quad \text{(A-17)}$$

The sum A-18 starting from $i = 3$ can be obtained from the values of derivatives of the function $T(z)$

$$\sum_{i=3} t_i z^i = T'(1) - T'(0) - T''(0) \qquad \text{(A-18)}$$

$$\text{where} T'(X) = \left[\frac{\partial T(z)}{\partial z}\right]_{z=X}, \quad T''(X) = \left[\frac{\partial^2 T(z)}{\partial z^2}\right]_{z=X}$$

Thus,

$$\begin{aligned} T'(1) &= n_A f_A \alpha_A (1 - v_{AB}) + n_B \alpha_B (1 - v_{BA}) \langle f_B \rangle_n \\ T'(0) &= n_A f_A \alpha_A (1 - v_{AB})(1 - \alpha_A + \alpha_A v_{AB})^{f_A - 1} \\ &\quad + n_B \alpha_B (1 - v_{BA}) \sum_j x_j f_{Bj} (1 - \alpha_B + \alpha_B v_{BA})^{f_{Bj} - 1} \end{aligned}$$

$$\begin{aligned} T''(0) &= n_A f_A (f_A - 1) \alpha_A^2 (1 - v_{AB})^2 (1 - \alpha_A + \alpha_A v_{AB})^{f_A - 2} \\ &\quad + n_B \alpha_B^2 (1 - v_{BA})^2 \sum_j x_j f_{Bj} (f_{Bj} - 1)(1 - \alpha_B + \alpha_B v_{BA})^{f_{Bj} - 2} \end{aligned} \qquad \text{(A-19)}$$

Finally, the concentration of EANCs in unit volume of the dry polymer, ν_e, is equal to

$$\nu_e = \frac{N_e \rho_p}{M_0} \qquad \text{(A-20)}$$

where ρ_p is specific gravity of the dry network and M_0 is the number-average molar mass of building unit

$$M_0 = n_A M_A + n_B \sum_j x_j M_{Bj}$$

References and Notes

(1) Dušek, K.; Dušková-Smrčková, M. *Prog. Polym. Sci.* **2000**, *25*, 1215–1260.
(2) Dušek, K.; Dušková-Smrčková, M. *Polymer networks* In *Macromolecular engineering*; Matyjaszewski, K., Gnanou, Y., Leibler, L., Eds.; Wiley-VCH: New York, 2007; Vol. *3*, pp 1687−1730.
(3) Stepto, R. F. T. *Polymer networks: principles of their formation, structure and properties*; Thomson Science: London, 1998.
(4) Erman, B.; Mark, J. E. *Structure and properties of rubberlike networks*; Oxford University Press: Oxford, U.K., and New York, 1997.
(5) Rubinstein, M.; Colby, R. H. *Polymer Physics*; Oxford University Press: Oxford, U.K., and New York, 2003.
(6) Suzuki, T.; Ikkai, F.; Shibayama, M. *Macromolecules* **2007**, *40*, 2509–2514.
(7) Keys, K. B.; Andreopoulos, F. M.; Peppas, N. A. *Macromolecules* **1998**, *31*, 8149–8156.
(8) Ilavský, M.; Dušek, K. *Macromolecules* **1986**, *19*, 2139–2146.
(9) Duračková, A.; Valentová, H.; Dušková-Smrčková, M.; Dušek, K. *Polym. Bull.* **2007**, *58*, 201–211.
(10) Vlasák, P.; Dušková-Smrčková, M.; Dušek, K. *J. Coat. Technol. Res.* **2007**, *4*, 311–315.
(11) Dušek, K. *Network formation by chain crosslinking (co)polymerization, in Developments in Polymerization. 3*; Haward, R. N., Ed.; Applied Science Publ.: Barking, U.K., 1982; pp 143−206.
(12) Dušek, K.; Galina, H.; Mikeš, J. *Polym. Bull.* **1980**, *3*, 19–25.
(13) Dušek, K.; Spěváček, J. *Polymer* **1980**, *21*, 750–756.
(14) Okay, O. *Polymer* **1999**, *40*, 4117–4129.
(15) Okay, O. *Prog. Polym. Sci.* **2000**, *25*, 711–779.
(16) Suzuki, T.; Shibayama, M.; Hatano, K.; Ishii, M. *Polymer* **2009**, *50*, 2503–2509.
(17) Sakai, T.; Matsunaga, T.; Yamamoto, Y.; Ito, C.; Yoshida, R.; Suzuki, S.; Sasaki, N.; Shibayama, M.; Chung, U. *Macromolecules* **2008**, *41*, 5379–5384.
(18) Matsunaga, T.; Sakai, T.; Akagi, Y.; Chung, U.; Shibayama, M. *Macromolecules* **2009**, *42*, 1344–1351.
(19) Matsunaga, T.; Sakai, T.; Akagi, Y.; Chung, U.; Shibayama, M. *Macromolecules* **2009**, *42*, 6245–6252.
(20) Matsunaga, T.; Sakai, T.; Shibayama, M. *Macromolecules* **2010**, *43*, 488–493.
(21) Dušek, K. In *Polymer networks. Structure and mechanical properties*; Chompff, A. J., Newman, S., Eds.; Plenum Press: New York, 1972, SBN-306-30544-5; pp 245−260.
(22) Gordon, M.; Scantlebury, G. R. *J. Polym. Sci., Part C: Polym. Symp.* **1968**, *16*, 3933–3942.
(23) Gordon, M.; Scantlebury, G. R. *J. Chem. Soc. B, London* **1967**, 1–13.
(24) Dušek, K.; Gordon, M.; Ross-Murphy, S. B. *Macromolecules* **1978**, *11*, 236–245.
(25) Dušek, K.; Vojta, V. *Br. Polym. J.* **1977**, *9*, 164–171.
(26) Sarmoria, C.; Miller, D. R. *Comput. Theor. Polym. Sci.* **2001**, *11*, 113–127.
(27) Sarmoria, C.; Valles, E. *Macromolecules* **1995**, *28*, 6244–6253.
(28) Cail, J. I.; Stepto, R. F. T.; Taylor, D. J. R. *Macromol. Symp.* **2001**, *171*, 19–36.
(29) Stepto, R. F. T.; Cail, J. I.; Taylor, D. J. R.; Ward, I. M.; Jones, R. A. *Macromol. Symp.* **2003**, *195*, 1–11.
(30) Lewin, L. A.; Douglas, C. B.; Dušek, K.; Dušková-Smrčková, M.; Vlasák, P. *Eur. Coat.* **2005**, *81*, 21–29.
(31) Ni, H.; Aaserud, D. J.; Simonsick, W. J., Jr.; Soucek, M. D. *Polymer* **2000**, *41*, 57–71.
(32) Duračková, A. Ph.D. Thesis, Inst. Macromol. Chem.,Prague/T. Bata Univ.: Zlin, CZ, 2008.
(33) Ahmed, Z.; Stepto, R. F. T. *Polym. J.* **1982**, *14*, 767–772.
(34) Semlyen, J. A., Ed. *Large ring molecules*; Wiley: Chichester, U.K., 1996; Chapter 16, pp 599−626, ISBN 0471967157.
(35) Suematsu, K. *Adv. Polym. Sci.* **2002**, *35*, 137–214.
(36) Dušková-Smrčková, M.; Dušek, K.; Vlasák, P. *Macromol. Symp.* **2003**, *198*, 259–270.
(37) Dušek, K.; Prins, W. *Adv. Polym. Sci.* **1969**, *6*, 1–102.
(38) Dušek, K. *Faraday Discuss. Chem. Soc.* **1975**, *57*, 101–109.
(39) Dušek, K. *J. Polym. Sci., Part C: Polym. Symp.* **1967**, *16*, 1289–1299.
(40) Flory, P. J. *Principles of Polymer Chemistry*; Cornell University Press: Ithaca, NY, 1951.
(41) Tompa, H. *Polymer solutions*; Butterworth: London, 1956.
(42) Andrews, R. D.; Tobolsky, A. V.; Hanson, E. E. *J. Appl. Phys.* **1946**, *17*, 352–359.
(43) Rubinstein, M.; Colby, R. H. *Macromolecules* **1994**, *27*, 3184–3190.
(44) Obukhov, S. P.; Rubinstein, M.; Colby, R. H. *Macromolecules* **1994**, *27*, 3191–3198.
(45) Sivasailam, K.; Cohen, C. *J. Rheol.* **2000**, *44*, 897–915.
(46) Colby, R. H.; Rubinstein, M. *Macromolecules* **1990**, *23*, 2753–2757.
(47) Dušek, K. *Adv. Polym. Sci.* **1986**, *78*, 1–59.
(48) Dušek, K.; *Networks from telechelic polymers: Theory and application to polyurethanes. in Telechelic polymers: Synthesis and applications*; Goethals, E. J., Ed.; CRC Press: Boca Raton, FL, 1989; pp 289−360.
(49) Dušek, K.; Dušková-Smrčková, M.; Fedderly, J. J.; Lee, G. F.; Lee, J. D.; Hartmann, B. *Macromol. Chem. Phys.* **2002**, *203*, 1936–1948.
(50) Dušek, K.; Dušková-Smrčková, M.; Yang, J.; Kopeček, J. *Macromolecules* **2009**, *42*, 2265–2274.
(51) Stockmayer, W. H. *J. Chem. Phys.* **1944**, *12*, 125–131.
(52) In the case of urethane network formation, it was shown that during the reaction (characterized by conversion of functional groups α), not only the concentration of EANCs increases, but also the interaction parameter χ increases. For this pseudoternary system,

$$\Delta\mu_1/RT = \ln a_1 = \ln \phi_1 + \phi_2 + \frac{\phi_3}{m_3} + \chi_{12}\phi_2^2 + \chi_{13}\phi_3^2$$
$$+ \left(\chi_{12} + \chi_{13} - \frac{1}{m_3}\chi_{23}\right)\phi_2\phi_3 + \nu_e V_{m1}[A\phi_2^{1/3}(\phi_2^0)^{2/3} - B\phi_2]$$

where $\phi_1 = 1 - \phi_2$ is the fraction of diluent, $m_3 = (V_{m3})_n/V_{m1}$ is the ratio of number-average molar volume of sol to the molar volume of the solvent and a_1 is the activity of the solvent; χ_{ij} are pair interaction parameters.